Hybrid nanocellulose decorated with silver nanoparticles as reinforcing filler with antibacterial properties

Amira Errokh, Albert Magnin, Jean-Luc Putaux, Sami Boufi

Hybrid nanocellulose decorated with silver nanoparticles as reinforcing filler with antibacterial properties

AmiraErrokh[a], Albert Magnin[b], Jean-Luc Putaux[c], Sami Boufi [a]*

[a]*University of Sfax- LMSE-Faculty of Science-BP 802-3018,Sfax, Tunisia*

[b]*Univ. Grenoble Alpes, CNRS, Grenoble INP, LRP, F-38000 Grenoble, France*

[c]*Univ. Grenoble Alpes, CNRS, CERMAV, F-38000 Grenoble, France*

* Corresponding author: e-mail : *sami.boufi@fss.rnu.tn*

Abstract

Cellulose (Cel) nanofibrils (CNFs) produced by periodate oxidation of native cellulose fibers were functionalized with silver (Ag) nanoparticles (NPs) using Tollens' reaction. The morphology and chemical composition of the resulting Cel-Ag hybrid nanofibrils were characterized using transmission electron microscopy (TEM), X-ray diffraction (XRD), as well as Fourier-transform infrared (FTIR) and UV-vis spectroscopies. To check whether the hybridization with Ag affected the reinforcing potential of the CNFs, nanocomposite films based on an acrylic matrix filled with the as-prepared Cel-Ag nanofibrils at different contents were processed by film casting. Their mechanical properties were investigated by dynamic thermomechanical analysis (DMTA). The hybrid Cel-Ag nanofibrils exhibited good bactericidal properties against $Gram^+$ and $Gram^-$ bacteria. Interestingly, the presence of Ag NPs did not seem to affect the reinforcing potential of the nanocellulose, and the amount of Ag leached out from films was below the permissible limit of 12 ppb. Nanocomposites based on this hybrid Cel-Ag nanofiller thus have great potential in the field of active packaging films, coating, and adhesives with enhanced antibacterial activity.

Published in: **Mater. Sci. Eng. C** 105 (2019), 110044

DOI: 10.1016/j.msec.2019.110044

1. Introduction

Periodate oxidation of cellulose (Cel) is a well-known reaction that selectively cleaves the C2–C3 bond of the glucopyranose unit forming two aldehyde groups per glucose unit [1]. The dialdehyde cellulose (DAC) has been long used as a precursor for cellulose derivatization in aqueous media to generate carboxylic, hydroxyl, imine, and amine functions, and for analytic purposes to identify sugars in polysaccharides [2]. Applied to cellulose fibers and cellulose nanofibrils (CNFs), periodate oxidation is an effective approach for grafting amines [3], dyes, and proteins [4] to further functionalize cellulose-based materials and extend their potential applications in catalysis, absorption [5] and reinforcement. Recently, it was shown that periodate oxidation of cellulose fibers could be used to produce nanocellulose with different morphologies, ranging from long nanofibrils to rod-like nanocrystals [6,7,8].

The hybridization of nanocellulose with metal and oxide nanoparticles (NPs) attracted increasing interest during this last decade [9,10]. The high surface area of nanocelluloses promotes a high loading of NPs with a size as low as 5 nm, their water stability in water allowing to avoid the use of organic solvents, and the wide range of target surface functionalization favoring the selective growth and anchoring of NPs on the surface of nanocellulose are as many benefits that drive for this increasing attention. The hybrid nanocelluloses have a broad potential as catalysts [2], biosensors [11], active packaging [12], wound dressing adsorbents [35], and in electronic devices.

More specifically, the hybridization of cellulose with silver nanoparticles (Ag NPs) has been the subject of extensive research with the objective to impart strong and durable antibacterial activity to cellulose, taking advantage of the bactericide property of Ag against a wide range of bacteria, fungi and viruses [13,14]. The immobilization of Ag NPs on nanocellulose prevents their aggregation during growth and reduces the risk of leaching out to the surrounding medium [15,16].

So far, three approaches have been developed to produce hybrid nanocellulose-Ag composites: (i) the addition of a reducing agent to the metal precursor in the presence of nanocellulose [12,17], (ii) the use of nanocellulose as both a reducing agent and immobilization substrate [18,19] and (iii) reduction via surface-functionalized nanocellulose [20]. The first approach is the simplest and consists in adding a conventional reducing agent such as $NaBH_4$, ascorbic acid or hydrazine, to a nanocellulose suspension in the presence of a solution of Ag precursor. However, this route is not selective and most of the Ag NPs will be formed in the solution with only a small fraction being generated on the surface of nanocellulose. The second approach relies on the use of nanocellulose as both support and reducer for the nucleation of Ag NPs taking advantage of the reducing capacity of hydroxyl groups. Although this approach is attractive, the direct evidence of the involvement of hydroxyl groups in the reduction process has not been confirmed yet, and the presence of functional groups such as carboxylic, sulfate, or amine is recommended to promote the coordination of Ag^+ ions

to the surface of nanocellulose. In addition, the reduction process must be activated at a temperature exceeding 80 °C. The third approach is based on the surface functionalization of nanocellulose with specific groups capable of being a reducing agent for ionic aqueous solutions of ionic silver. Considering that the reduction process occurs on the surface of the substrate, we expect the nucleation and growth of Ag NPs to take place selectively on the surface of nanocellulose. This will ensure the effective anchoring of the Ag NPs on the surface of nanocellulose, avoid formation of free Ag NPs in solution and allow for a better control of the Ag NP size.

Recently, several works have pointed out the possibility to use hybrid nanocellulose-Ag as an active bifunctional filler that takes advantage of the presence of Ag NPs imparting a bactericidal effect while nanocellulose provides reinforcement. Li et al. have used dialdehyde nanofibrillated cellulose (DATNFC) as a template for the deposition of silver nanoparticles (DATNFC@Ag) without the addition of a reducing agent [21]. Paper films prepared by vacuum filtration showed excellent mechanical properties and exhibited efficient antibacterial activity against both *Staphylococcus aureus* and *Escherichia coli*. Hybrid carboxylated cellulose nanocrystals (CCNs) and Ag NPs were prepared by adsorption of Ag^+ ions followed by reduction with $NaBH_4$ and were included in a waterborne polyurethane matrix as reinforcing and antibacterial nanofiller [22]. Another work reported the use of cellulose nanocrystals/silver as bifunctional reinforcement in poly(3-hydroxybutyrate-co-3-hydroxyvalerate) (PHBV) matrix [23]. The nanocomposite films prepared by solvent casting exhibited better thermal stability and mechanical properties than the neat matrix and an effective antibacterial activity against both *Gram- E. coli* and *Gram+ S. aureus* was observed. However, the hybridization process was carefully controlled by tailoring the number of appended Ag NPs and their size to avoid losing the intrinsic reinforcing potential of the nanocellulose.

In the present work, hybrid Cel-Ag nanofibrils were produced by the periodate oxidation of bleached cellulose fibers followed by treatment with a$AgNO_3$ solution under basic conditions. The periodate oxidation was simultaneously used as a pre-treatment to facilitate the breakdown of cellulose fibers into nanofibrils and to generate aldehyde functions used as reducing agents for the growth of Ag NPs. Then, nanocomposite films were prepared by mixing the Cel-Ag nanofibrils with an acrylic polymer latex were prepared to investigate how the hybridization of CNFs affected the reinforcing properties of the nanocellulose. The impact of the presence of silver in the nanocomposite to prevent bacterial growth on the surface of the film was also evaluated.

2. Experimental section

2.1. Materials

Chips from *Eucalyptus grandis* wood (approximately 1×0.5×0.2 cm^3) were used to prepare cellulose pulp. Sodium periodate ($NaIO_4$), lithium chloride (LiCl), silver nitrate ($AgNO_3$, 99.9 %),

sodium hydroxide (NaOH), and ammonium hydroxide (NH_3OH, 25%) were purchased from Aldrich and used as received.

2.2. Fibers extraction

The milled wood chips were pulped at a solid content of 10 wt% with a 4 wt% NaOH solution for 2 h at 70-80 °C under mechanical stirring. This treatment was repeated three times until the fibers were well individualized. The resulting fibers were subsequently filtered and rinsed with distilled water and twice bleached with $NaClO_2$ to remove the residual lignin. The bleaching treatment was carried out at 70 °C for 1h at pH 4.8. The solution was composed of equal parts of aqueous chlorite (1.7 wt% $NaClO_2$ in water) and acetate buffer.

2.3. Periodate oxidation of cellulose fibers

Periodate oxidation of cellulose fibers was performed as follows: 2.5 g of fibers was mixed with 200 mL of 1% sodium metaperiodate solution (0.6 mol for 1 mol of glucopyranose) containing 0.3 g of LiCl and left under stirring under dark during 48 h at 40 °C. Then, the reaction was stopped by adding 1 g ethylene glycol to decompose the residual $NaIO_4$ and the oxidized fibers were thoroughly washed with water by filtration. The aldehyde content of oxidized fibers was determined by converting the aldehyde function into oxime after reaction with hydroxylamine hydrochloride and titration of forming HCl obtained from oxime reaction between the NH_2OH. HCl and aldehyde groups. The oxidized cellulose was recovered and purified by three consecutive centrifugation/washing cycles to remove ionic residues. The yield in nanosized material at this degree of oxidation and after 2 min sonication was found to be around 80%, which is in agreement with our previous work [24].

2.4. Preparation of Tollens' reagent

Silver nitrate (0.2 M) and NaOH (0.2 M) solutions were mixed, resulting in Ag_2O brown powder precipitation. The Ag_2O was dissolved by adding a 2 wt% aqueous ammonium solution to the mixture, dropwise and under magnetic stirring. The brown powder gradually disappeared leading to the preparation of silver ammonium complex $Ag(NH_3)_2^+$ (Tollens' reagent).

2.5. Preparation of Cel-Ag

One gram of oxidized cellulose fibers was suspended in 50 mL water and was heated at 80 °C for 1h. Then, the suspension was sonicated for 2 min using a 24 kHz Branson digital Sonifier S-450D (Germany) coupled with a horn (tip diameter of 13 mm). After sonication, the cellulose suspension became translucid, indicating the breakdown of the cellulose fibers into nanosized fibrils. To nucleate Ag NPs, 30 mL of the as-prepared Tollens reagent was added to the sonicated suspension and kept under magnetic stirring at 50 °C for 30 min. immediately after the addition of Tollens' reagent, the cellulose suspension turned to green-brown with intensification of the color with time. The Cel-Ag

was recovered by centrifugation at 8000 rpm for 20 min, redispersed in water, and centrifuged three times to remove the remaining salts. Finally, the Cel-Ag was dialyzed against distilled water to remove any residual $Ag(NH_3)_2^+$or Ag^+. This was verified by the neutrality of the dialysis effluent.

2.6. Preparation of the nanocomposites

The nanocomposite films were prepared by mixing a suspension of Cel-Ag nanofibrils at different contents with commercial acrylic latex produced by the copolymerization of styrene (S) and butyl acrylate (BuA) having a glass transition around 20 °C, followed by casting in a Teflon mold. The mixture was left at 40 °C for two days until complete evaporation of water and film-formation by coalescence of polymer particles. A light brown translucid film was obtained with a thickness between 300 to 400 µm.

2.7. X-ray diffraction (XRD)

Strips of films dried at 50 °C were X-rayed in reflection mode with a CuK_α radiation (λ = 0.1542 nm) generated in a Bruker AXS diffractometer (Madison, WI, USA) at 30 kV and 100 mA, from 5 to 70°, with a scanning step of 0.05° and a step time of 10 s.

2.8. Fourier-transform infrared spectroscopy (FTIR)

FTIR spectra were recorded using a Perkin Elmer FT-IR Spectrum 100 equipped with an attenuated total reflectance (ATR) Ge/Ge accessory.

2.9. Dynamic thermomechanical analysis (DMTA)

DMTA experiments were carried out with a PYRISTM Diamond DMA (Perkin-Elmer, Waltham, MA), working in tension mode. Samples, with dimensions of about 20 mm (length) by 5 mm (width) and 0.2 mm (thickness) were heated from -20 to 120 °C with a heating rate of 2 °C.min^{-1} at a frequency of 1 Hz and an amplitude of 10 µm. The storage (E') was measured as a function of temperature.

2.10. Thermal analysis

The thermogravimetric analysis (TGA) was performed with a TGA 400 thermogravimetric analyzer (Perkin Elmer, France) from 20 to 800 °Con 10 mg samples, at a heating rate of 10 °C.min^{-1} under airflow.

2.11. Transmission electron microscopy (TEM)

Droplets of dilute Cel-Ag suspensions were deposited on freshly glow-discharged carbon-coated copper grids and allowed to dry after negative staining with 2wt% uranyl acetate. The specimens were observed with a JEOL JEM-2100Plus microscope operating at 200 kV and images were recorded using a Gatan Rio 16 camera. The size of the Ag nanoparticles was measured from the images using the ImageJ software.

2.12. UV-vis spectroscopy

Absorption spectra were recorded from 200 to 800 nm using a Lambda 35 UV-visible spectrometer (Perkin-Elmer).

2.13. Inhibition test for antimicrobial activity

The antimicrobial assay was run using the disc diffusion method tested against *Enterococcus faecali* (ATCC 29212) and *Micrococcus luteus* (ATCC 4698) chosen as (Gram+) bacterium and *E. coli* (ATCC 25922) as (Gram-) bacterium, using the disc diffusion method on an agar plate following the method reported by Barry et al. [36]. The bacteria were first cultured in a flask with 9 mL of LB. The incubation was performed at 37 °C and oscillated at a frequency of 200 rpm for 18 h. Then, 100 µL of each culture suspension of all tested bacteria with a concentration of 106 CFU/mL was spread on the agar plates. The nanocomposite films were cut into circular pieces (1 cm diameter), sterilized in an autoclave at 121 °C for 20 min, and kept in intimate contact with the bacterial agar gel. After incubation for 24 h at 37 °C, samples were visually examined for the growth of bacteria in the area surrounding the film.

2.14. ICP-OES analysis of released silver in solution.

Composite films (4×4 cm^2) containing Cel-Ag nanofibrils were left in a 100 mL water/ethanol mixture (50/50 v/v) for 24 h under shaking and the total Ag content was evaluated by inductively coupled plasma optical emission spectrometer (PerkinElmer Optima7300 DV ICP-OE) after acidifying with nitric acid.

3. Results and discussion

3.1. Preparation of Cel-Ag hybrid nanofibrils

The aldehyde-functionalized nanocellulose with an aldehyde content of 1280 µmol.g^{-1} was produced by periodate oxidation of never-dried cellulose fibers followed by heating at 80 °C for 1 h and a short sonication treatment (2 min) to ensure the complete breakdown of cellulose fibers into nanofibrils. After this treatment, a translucid suspension was obtained, which is in agreement with our previous work [24] and that was reported by Yang et al. [5]. Immediately after the addition of the $Ag(NH_3)_2^+$ solution, the suspension of oxidized cellulose turned to green-brown without any visible sign of aggregation, as attested by the absence of sedimentation and by the translucent aspect of the suspension(**Fig. 1A**).The UV-Vis spectrum of the suspension (**Fig. 1B**) showed a strong absorption peaking at 425 nm which is typical of the surface plasmon resonance (SPR) of Ag nanoparticles [25].

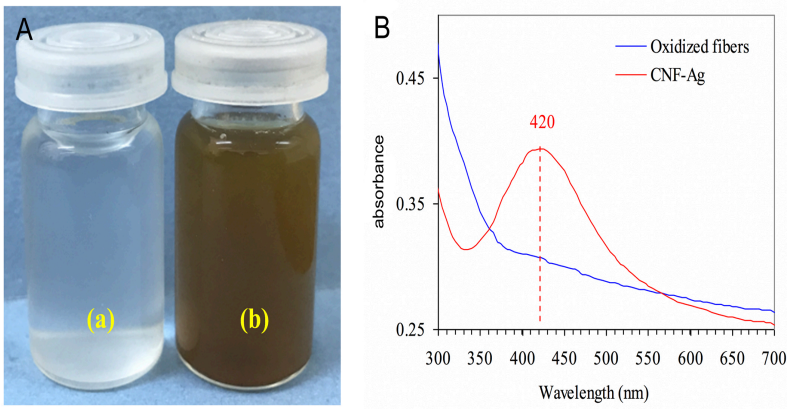

Fig.1:A) Photograph of oxidized fibers CNFs (a) and Cel-Ag (b) suspensions at an 0.5 wt% solid content; B) UV-Vis spectra of oxidized fibers and Cel-Ag suspension in water.

The formation of Ag NPs was confirmed by XRD analysis of a Cel-Ag film. In addition to the native cellulose I diffraction peaks at 2θ= 16.2, 22.4, and 34.6°, the XRD profile contains the typical diffraction peaks of Ag at 2θ = 38.2, 44.4° and 64.6° corresponding to (111), (200) and (220) planes of the face-centered cubic (*fcc*) structure of metallic Ag (JCPDS no. 04-0783) (**Fig. 2**). The presence of these new peaks confirms the generation of metallic Ag in Cel-Ag. Moreover, the relatively large width of the Ag diffraction peaks is indicative of a small crystallites size. Using Scherrer's equation $d = K\lambda/\beta\cos\theta$, where λ is the radiation wavelength, θ half the diffraction angle, β is the peak width at half-height, and K, a constant generally taken as 0.9, the size of the Ag crystallites was estimated to be around 13 nm. Compared to neat cellulose fibers, a decrease in the crystallinity of the CNFs produced by periodate oxidation was noted as attested by the increase in the intensity scattered by the amorphous part at 2θ around 18°, which was expected assuming that the opening of glucopyranose rings after periodate oxidation results in the disruption of the packing order of cellulose chains in the crystalline domains. This result agrees with our previous and work in literature data [1,24].

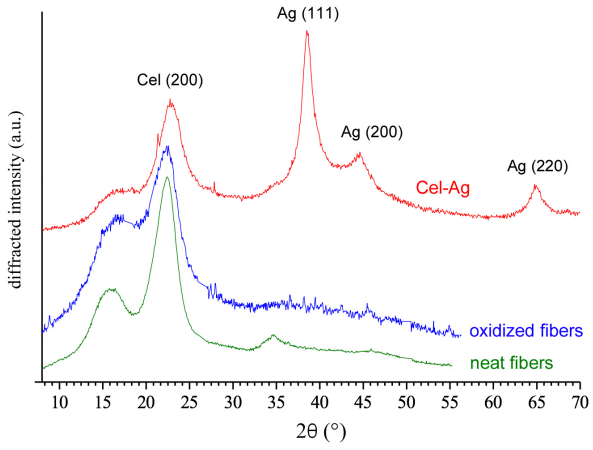

Fig. 2: XRD profiles of neat cellulose fibers (green), $NaIO_4$-oxidized fibers (blue), and hybrid Cel-Ag nanofibrils after Tollens' reaction (red).

The ATR-FTIR spectra of neat and oxidized fibers, as well as Cel-Ag nanofibrils are shown in Fig. 3. After periodate oxidation, the main evolution corresponds to the emergence of two bands at 1725 and 875 cm-1 assigned to the carbonyl group stretching and the hemiacetal linkages formed from the dialdehyde group, respectively. The main characteristic bands of the cellulose skeleton at around 1155, 1100, and 1045 cm^{-1} corresponding to the C–O–C asymmetric stretching, ring asymmetric stretching, and C–O stretching, respectively, remained roughly unchanged, but were less sharp after oxidation, which is presumably due to the reduction in the crystallinity degree of cellulose. After the treatment with the $AgNO_3$ solution, the intensity of the carbonyl band at 1725 cm^{-1} decreased, confirming the involvement of aldehyde groups in the reduction process. However, the formation of carboxylic groups in Cel-Ag which may overlap with the band at 1630 cm^{-1} corresponding to adsorbed water, cannot be unambiguously confirmed. The hemiacetal band at 875 cm^{-1} is absent, confirming again the consumption of the aldehyde groups during the interaction with $Ag(NH_3)_2^+$.

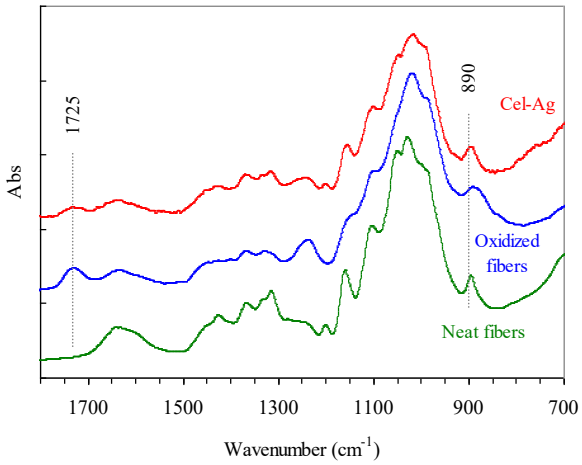

Fig. 3: ATR-FTIR spectra of neat fibers, oxidized fibers and Cel-Ag nanofibrils.

The production of hybrid Cel-Ag, starting from cellulose fibers would thus involve the following steps:

1) The cellulose nanofibrils constituting the cellulose fibers were oxidized generating dialdehyde groups, the content of which is controlled by the cellulose/$NaIO_4$ weight ratio.

2) The cellulose fibers were broken down into nanosized fibrils after heat treatment and gentle sonication of oxidized fibers. The fiber suspension became translucid after this treatment, indicating the disruption of the micron-sized fibers. This approach is based on the work of Van de Ven and our previous work [24] and we assume that the periodate oxidation preferentially affects the disorganized regions and the surface layer of the crystalline segments. Upon heating and ultrasonication, the disorganized regions would disintegrate giving rise to hairy cellulose fibrils sterically stabilized by dangling chains protruding from the crystalline regions [26]. However, it is worth noting that the

generation of cellulose nanofibrils by this approach is not systematic and seems to depend on the origin of cellulose pulps as well as the extent of the oxidation. So far, the disintegration of cellulose fibers was observed only for never-dried specimens, while dried fibers did not show any marked change in their aspect after the same treatment.

3) Reduction of Ag ions into Ag^0 nucleus that self-aggregated on the surface of the CNFs giving rise to metallic Ag NP. The binding of Ag NPs on the surface of CNFs can be explained by the adsorption of $Ag(NH_3)_2^+$ on the surface of the fibrils and by their intimate contact with the aldehyde group during the electron transfer process from the CO to $Ag(NH_3)_2^+$. Once formed, the Ag^0 nuclei aggregate to form Ag NPs immobilized on the surface of the nanofibril.

The reduction of silver ions is caused by the transfer of electrons from the reducing agent (presently aldehyde or hemiacetals at the surface of CNFs) to the oxidized metallic species $Ag(NH_3)_2^+$ as shown in Scheme 1. This reaction known as Tollens' test is selective for aldehydes and occurs under alkaline aqueous conditions in the presence of ammonia. The addition of ammonia is necessary to prevent the precipitation of brown Ag_2O by coordination of Ag^+ with. However, this coordination lowered also the redox potential of Ag precursor, moving from +0.799 for Ag^+/Ag ($E^0_{Ag^+/Ag} = +0.799$) to +0.38 V for $[Ag(NH_3)_2]^+$ ($E^0_{[Ag(NH3)2]+/Ag} = +0.38$ V) [27]. This decrease in the redox potential contributes to controlling the nucleation and growth of metallic Ag NPs by reducing the kinetics of generation of metallic Ag^0 nuclei on the surface of nanofibrils. Aside from providing the reducing entity for $[Ag(NH_3)_2]^+$, the cellulose nanofibrils also act as a stabilizing agent preventing the ensuing Ag NPs from aggregation, keeping the Cel-Ag suspension colloidally stable.

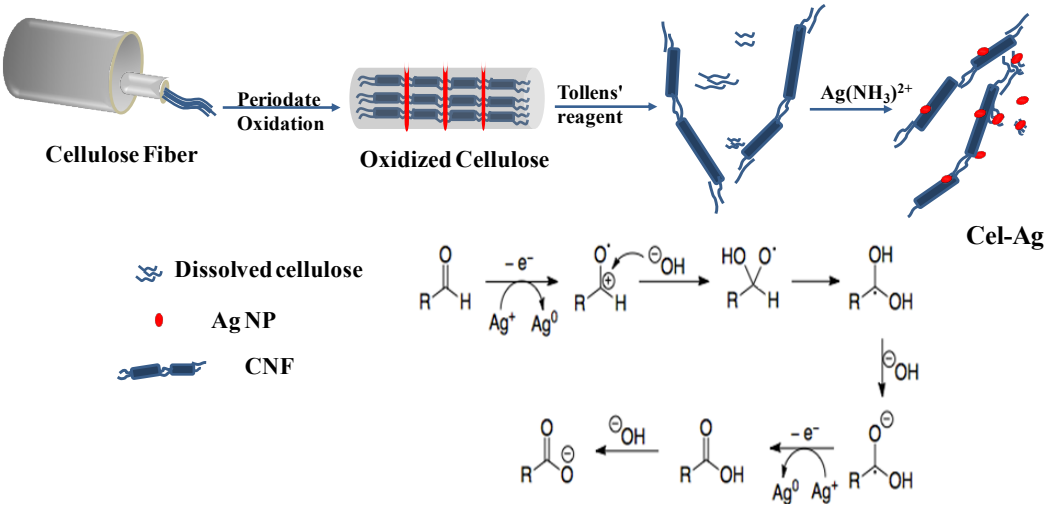

Scheme 1. Illustration of the different steps involved in the production of Cel-Ag using Tollens' reaction.

The thermal stability of Cel-Ag was assessed by TGA and thermograms are shown in **Fig. 4**. The neat cellulose fibers exhibit a two-step degradation profile starting at around 300 °C and followed by

a second step at 350 °C. The first event corresponds to the cleavage of the glycosidic bond and the second step to the oxidative degradation of the carbonaceous residue. The periodate oxidized cellulose has a lower thermal decomposition onset at around 200 °C which has been also reported by other authors [28]. The shift toward lower degradation temperatures has been explained by the lower crystallinity of the oxidized samples and degradation reactions during periodate oxidation [29]. Presumably, the destruction of ordered packaging of cellulose molecules following the opening of the glucopyranose ring by the oxidation reaction facilitated the thermal scission of covalent bonds and the generation of volatile products. However, other phenomenon might occur following the hybridization process as has been observed in nanocellulose-silica hydrogels [36]. The thermal degradation profile of Cel-Ag is between that of neat cellulose and oxidized cellulose with a slower decomposition rate and better thermostability than neat cellulose at a temperature higher than 350 °C. The ash content in Cel-Ag was low (around 1 wt%), indicating that the amount of appended Ag on CNFs was quite low and did not exceed 1 wt%.

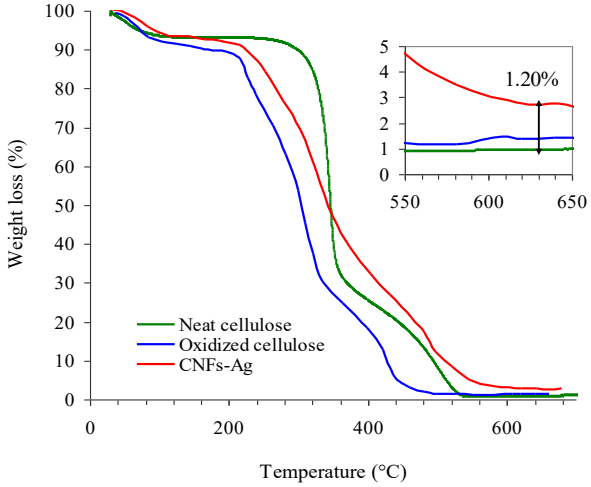

Fig. 4: TGA thermograms for neat cellulose fibers, oxidized fibers, and Cel-Ag nanofibrils.

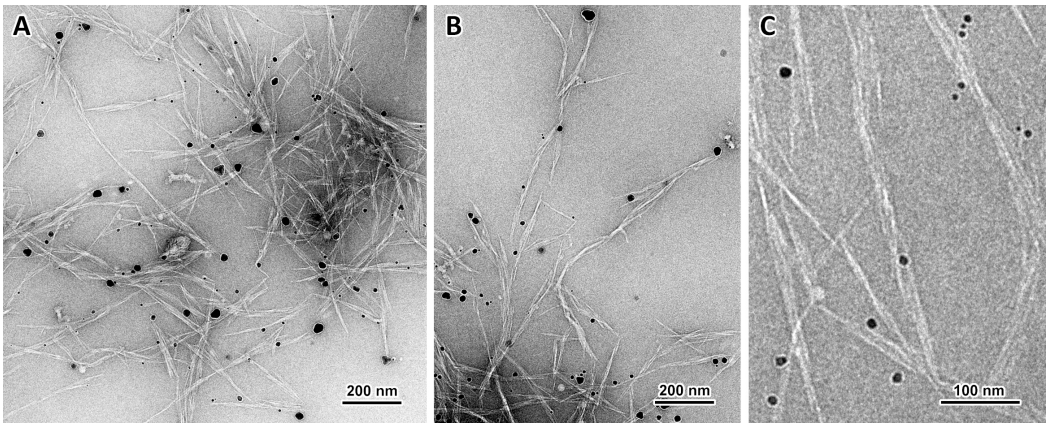

Fig. 5: A-C) TEM micrographs of negatively stained Cel-Ag hybrid nanofibrils. Image C is displayed at a higher magnification to show some of the smallest nanoparticles attached to cellulose.

3.2. Morphology of Cel-Ag nanofibrils

The TEM images in **Fig. 5** shows generally bundled Cel-Ag nanofibrils with a length in the micron range. Some, but not all, carry a few Ag NPs on their surface that are polydisperse, with a size ranging between 5 and 50 nm. The larger NPs are clearly polygonal. Very little NPs were observed not attached to CNFs, and no aggregation could be seen on the surface of the nanofibrils. If we assume that aldehyde groups were evenly distributed along the CNF surface and that each of them has generated two atoms of Ag^0during Tollens' reaction, then we should expect a more significant surface covering of the CNFs by Ag NPs. A possible reason accounting for the limited number of Ag NPs on CNFs might be the higher concentration of aldehyde groups at the extremity of the crystallite domains being more accessible. However, the exact location of the Ag NPs could not be determined with precision from the TEM images as the CNFs were generally bundled. Ag NPs may have also been formed by reduction with aldehyde groups located in disorganized domains along CNFs, at kinks, for instance.

3.3. Nanocomposite films reinforced with Cel-Ag nanofibrils

CNFs are known to impart strong reinforcing effect to polymer matrices provided that the nanofibrils are well-dispersed [30]. However, a good dispersion of the filler is hard to achieve without surface modification when melt processing route was adopted and dry nanocellulose is used. To address the question of the extent to which the hybridization of CNFs with Ag NPs is likely to affect the reinforcing potential of CNFs, nanocomposite films were prepared using solvent casting after mixing with a polymer latex dispersion. Nanocomposite films with a Cel-Ag nanofibril content ranging from 1 to 10 wt% were prepared and their mechanical properties studied by DMAT analysis over a temperature range spanning from the glass region to the rubbery domain. The evolution of the storage modulus (E') with temperature at different Cel-Ag contents is shown in **Fig. 6**. Below the glass transition, E' remained nearly unchanged while, above the glass transition, the effect of the addition of Cel-Ag was much more obvious, with a strong increase in storage modulus, all the more important as the content in the nanofiller increased. This marked increase of E' clearly indicated that the CNFs holding Ag NPs did not lose their reinforcing effect.

To better highlight the stiffening effect of the Cel-Ag nanofibrils, the increment in E' with respect to the neat matrix ($I = E_n^{'} / E_m^{'}$) (E'_n and E'_m correspond to the storage modulus of the nanocomposite and neat matrix at 70 °C, respectively) in the rubbery state (T_g=40°C) versus Cel-Ag content was plotted. A steady increase in the increment with Cel-Ag content was observed up to 6 wt% nanofiller loading, confirming the effective reinforcing potential of the hybrid CNFs. For instance, at a content of 6 wt%, the increase in modulus was about 200 times that of the neat matrix. Interestingly, when compared to the CNFs without Ag, the presence of Ag appended to the CNFs did not impede the

reinforcing potential up to 6 wt%. Both of the pristine CNFs and hybrid Cel-Ag nanofibrils exhibited nearly the same trace in the increment of the modulus. However, over a critical level between 6-8 wt%, the increment in the modulus leveled off, indicating a decrease in the reinforcing effect of Cel-Ag nanofibrils. A possible reason of this effect might be the aggregation of Cel-Ag nanofibrils as their amount exceeded a certain amount.

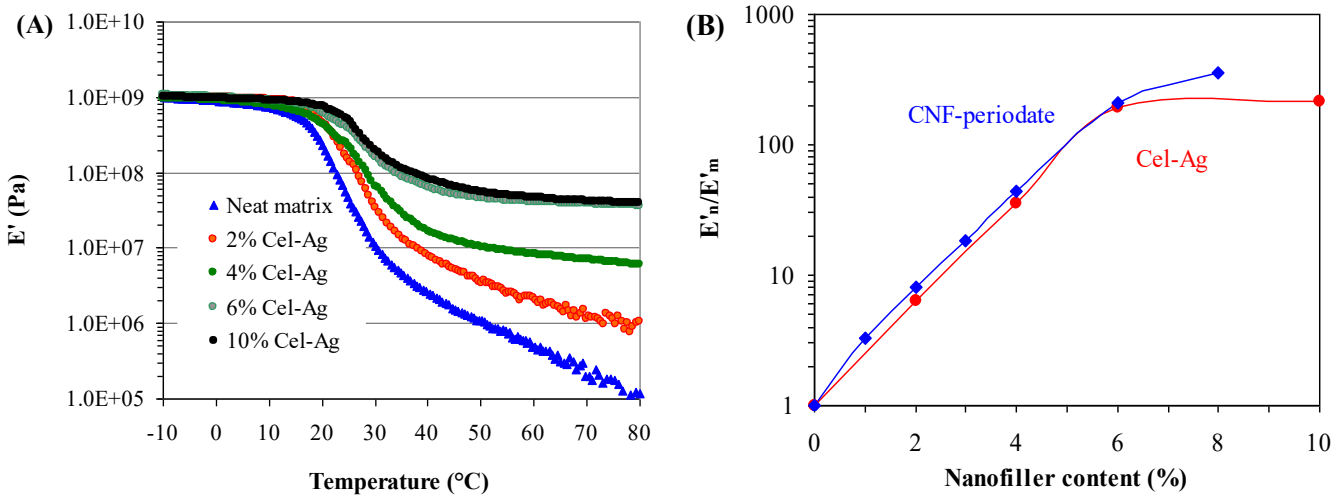

Fig. 6: (A) Storage tensile modulus, *E'*, *vs.* temperature at 1 Hz and (B) evolution of the increment in modulus *vs.* Cel-Ag content at 70 °C.

3.4. Antibacterial properties

The antibacterial activity of Ag NPs is well recognized with an efficiency that increases as the particle size decreases [31]. Given the outstanding bactericidal activity of Ag NPs against both *Gram+* and *Gram-* bacteria as well as fungi and viruses at low dosage [32], the hybridization of CNFs with Ag NPs is expected to confer them antibacterial properties in addition to their strong reinforcing capacity when incorporated into a polymer matrix.

The antibacterial activity was first assessed with thin dry films of oxidized CNFs and Cel-Ag nanofibrils, using the disk-diffusion method with *E. faecali* and *Micrococcus* as *Gram+* bacteria and *E. coli* as *Gram-* bacteria (**Fig. 7**). The oxidized CNFs exhibited no antibacterial activity which was expected given the known sensitivity of cellulose to bacterial attack. By contrast, the film of Cel-Ag nanofibrils showed a clear inhibition zone against *E. faecali* and *E. coli*, indicating substantial antibacterial activity. The activity of Cel-Ag was attributed to the presence of AgNPs tightly bound to cellulose nanofibrils which may result from different mechanisms: (i) interaction of Ag with the bacteria's outer membrane, inducing structural changes that lead to cell death, (ii) interaction of released silver ions with sulfur and phosphorus in DNA resulting in the inactivation of the DNA replication, (iii) the generation of reactive oxygen species (ROS) catalyzing the destruction of bacteria [33]. However, the mechanism of antibacterial action of AgNPs is still a matter of debate.

The antibacterial activity of Cel-Ag nanofibrils, incorporated into a polymer matrix, was also evaluated to check whether Cel-Ag was still active when the nanofiller was buried inside a polymer matrix. The same method was used by replacing the pure Cel-Ag film by a nanocomposite film containing different content in Cel-Ag. **Fig.7** presents the pictures of the diffusion assay resulting from neat matrix film and matrix-Cel-Ag nanocomposite films with 6 wt% Cel-Ag loading. On the one hand, neat matrix films did not show any inhibitory effects on all the bacterial tested as confirmed with the spreading of microorganisms in the surrounding environment. On the other hand, for nanocomposite films with 6 wt% Cel-Ag loading, a better antibacterial activity was observed as confirmed by the appearance of an inhibition zone around the film. The absence of a large inhibition zone is probably due to the immobilization of antibacterial Ag NPs on the polymer matrix reducing the possibility of direct contact with bacteria as well as the amount of released silver in the surrounding environment. Seemingly, the antibacterial activity is higher for Gram+ bacteria than Gram- which might be due to the differences in their structural and chemical cell membrane compositions. However, more work is needed to better investigate how the type of bacteria behaves in contact of Cel-Ag hybrid material. Even though silver nanoparticles are considered promising nanomaterials in medical applications and biotechnology, their mechanism of action is still a matter of debate.

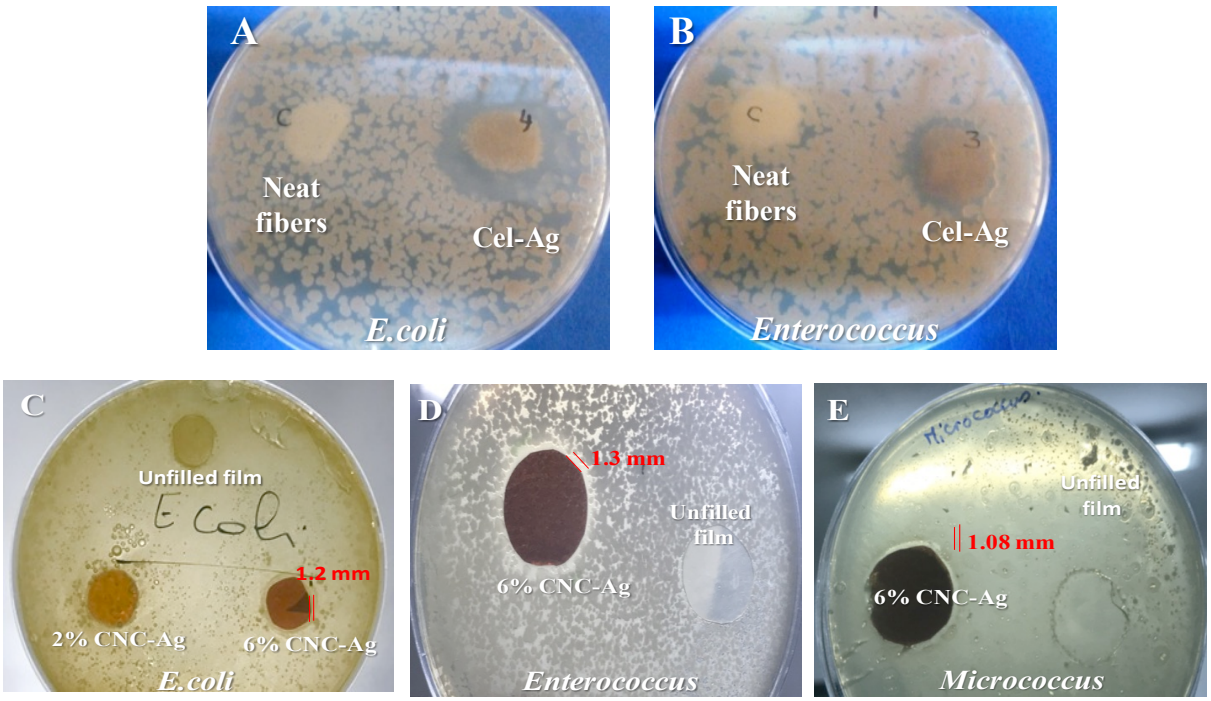

Fig. 7. Antibacterial behavior of, neat fibers (dried), Cel-Ag dried (A,B) neat matrix polymer and nanocomposite films containing 2% and 6 wt% Cel-Ag (C) and 6 wt% Cel-Ag (D,E), using the disk-diffusion method.

Another approach was tested to confirm the antibacterial potential of nanocomposite films. Film samples were immersed in microbial suspension with an initial number of bacteria of 10^5 CFU.mL^{-1} (*S. aureus*) for 2 h, then they were removed dried at room temperature for 1h and incubated in an agar plates during 24 h at 37 °C. The aspect of the plate for the neat matrix and nanocomposite with 2 and 6 wt% Cel-Ag is shown in **Fig. 8**. On the one hand, for the neat matrix, bacterial growth can be seen at the periphery of the film, indicating that bacteria remained alive and bound to the film after drying. On the other hand, bacterial growth was very limited on nanocomposite films with 2 and 6 wt% Cel-Ag, with only limited area of growth around the film. This suggests that most bacteria in contact of the nanocomposite films containing Cel-Ag have been killed as the film was left to dry. This antibacterial activity can be explained by two mechanisms; (i) the first one is the release of Ag^+ from Ag NPs, and (ii) the presence on the film of Ag NPs migrating to the surface acting as antibacterial agent. The binding of Ag NPs on the CNFs would reduce their tendency to aggregate during film formation and would favor the effective dispersion within the polymer matrix. Moreover, as the Ag NPs are bound to the CNFs, the risk of leaching out from the film will be strongly reduced.

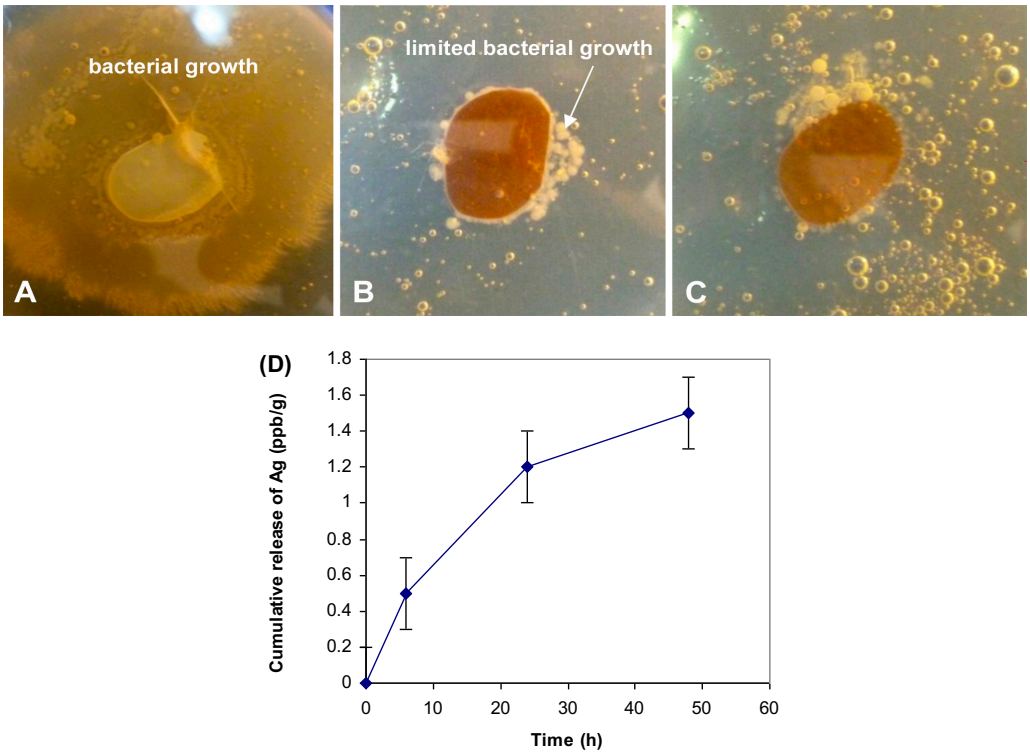

Fig. 8: Antibacterial activity test against *Staphylococcus aureus* of neat matrix (A), nanocomposite with 2 wt% (B) and 6 wt% (C) Cel-Ag nanofibrils. (D) Ag release profile for a nanocomposite film with 10% Cel-Ag content in water/ethanol (50/50 v/v) mixture.

3.5. Release of silver from nanocomposite films

In material containing Ag NPs, the leaching out of Ag in the surrounding medium, either in the form of NPs or ionic species by dissolution is a key concern and care should be taken to avoid

excessive release of Ag, beyond an acceptable threshold. Referring to US National Institute for Occupational Safety and Health (NIOSH), the recommended permissible exposure limit is 10 ppb for all forms of silver [34]. To evaluate the amount of leached Ag from nanocomposite film containing 10% Cel-Ag, a sample (4×4 cm^2) was left in 100 mL water/ethanol mixture (50/50 v/v) for 48 h under shaking and the total silver was evaluated by ICP which measures total silver content (i.e., silver ions and nanoparticles). The evolution of the amount of released silver with time is shown in **Fig. 8**. It reached 0.5, 1.2, and 1.6 ppb after 6, 24, and 48 h, respectively, which is well below the permissible limit. This slow and low silver leaching can be explained, on the one hand, by the low content in Ag bound to the Cel-Ag nanofibrils and, on the other hand, by the embedding of Cel-Ag within the polymer matrix, which generates a hydrophobic barrier layer against the dissolution of Ag from the NPs. This could explain the small inhibition halo observed in the disk diffusion method for Cel-Ag-polymer nanocomposite films.

Although the amount of released Ag might depend on the stimulus, this result is encouraging and opens the way toward the potential applications of Cel-Ag hybrid nanofibrils in active packaging or bactericidal coating films.

4. Conclusions

CNFs functionalized with Ag NPs have been produced by a two-step process, starting from never-dried bleached pulps, $AgNO_3$ as a precursor for silver, and water as the sole solvent. The process involved the periodate oxidation of the pulp to generate aldehyde groups and facilitate the breakdown of the cellulose fibers into nanosized cellulose. Then, an $AgNO_3$ solution with ammonia was added to the oxidized fibers suspension in water without any external reducing agent. The generation of Ag NPs was based on the well-known Tollens reaction, exploiting the aldehyde function on cellulose to reduce $Ag(NH_3)_2^+$ into metallic Ag. The formation of metallic Ag NPs was confirmed by XRD showing the diffraction peak of Ag and by UV-Vis revealing a strong absorption at 420 nm, typical of the plasmon of Ag NPs. TEM observation confirmed the binding of Ag NPs on the surface of CNFs, with an average particle size lower than 20 nm. Moreover, free Ag NPs were observed whose presence was explained by the dissolution of a fraction of cellulose in water following the oxidation reaction.

The inclusion of hybrid Cel-Ag nanofibrils into a polymer matrix by mixing the Cel-Ag suspension with a polymer latex followed by casting and film formation at room temperature produced a brown translucid nanocomposite film with an effective capacity to prevent the growth of bacteria on the surface of the film. Moreover, the presence of Ag was shown not to affect the reinforcing potential of CNFs up to a 6 wt% loading. This finding contributes to further extend the potential application of nanocellulose as a reinforcing agent with high resistance to bacterial growth.

Acknowledgments

This work has been partially supported by the LabEx Tec 21 (Investissements d'Avenir – grant agreement #ANR-11-LABX-0030). LRP and CERMAV are part of Institut Carnot PolyNat (Investissements d'Avenir – grant agreement #ANR-11-CARN-030-01). The authors acknowledge the Glyco@Alps program (Investissements d'Avenir – grant agreement #ANR-15-IDEX-02) for financial support and thank the NanoBio-ICMG Platform (FR 2607, Grenoble) for granting access to the Electron Microscopy facility. The PHC Utique19G1123 is also acknowledged.

References

[1] P. Calvini, A. Gorassini, G. Luciano, E. Franceschi, FTIR and WAXS analysis of periodate oxycellulose: Evidence for a cluster mechanism of oxidation, Vib. Spectrosc. 40 (2006) 177−183.

[2] E. Lam, S. Hrapovic, E. Majid, J.H. Chong, J.H.T. Luong, Catalysis using gold nanoparticles decorated on nanocrystalline cellulose, Nanoscale 4 (2012) 997–1006.

[3] E. Maekawa, T. Koshijima,Preparation and structural consideration of nitrogen containing derivatives obtained from dialdehyde celluloses. J. Appl. Polym. Sci. 42(1991) 169−178.

[4] A.E. Gurvich, E.V. Lechtzind, High capacity immune adsorbents based on preparations of reprecipitated cellulose, Mol. Immunol. 19(1982) 637–640.

[5] J.S. Kim, E. Kuk, K.N. Yu, J.H. Kim, S.J. Park, H.J. Lee, S.H. Kim, Y.K. Park, Y.H. Park, C.Y. Hwang, Y.K. Kim, Y.S. Lee, D.H. Jeong, M.H. Cho, Antimicrobial effects of silver nanoparticles, Nanomedicine 3 (2007) 95–101.

[6] H. Yang, M.N. Alam, T.G.M. Van de Ven, Highly charged nanocrystalline cellulose and dicarboxylated cellulose from periodate and chlorite oxidized cellulose fibers, Cellulose 20(2013) 1865−1875.

[7] H. Liimatainen, M. Visanko, J.A. Sirviö, O.E.O. Hormi,J. Niinimaki, Enhancement of the nanofibrillation of wood cellulose through sequential periodate−chlorite oxidation, Biomacromolecules 13 (2012)1592−1597.

[8] J. Leguy, A. Diallo, J.-L. Putaux,Y. Nishiyama, L. Heux, B. Jean, Periodate oxidation followed by $NaBH_4$reduction converts microfibrillated cellulose into sterically stabilized neutral cellulose nanocrystal suspensions, Langmuir 34(2018)11066−11075.

[9] M. Kaushik, A. Moores, Review: Nanocelluloses as versatile supports for metal nanoparticles and their applications in catalysis. Green Chem. 19 (2016) 622–637.

[10] M. Rezayat, R.K. Blundell, J.E. Camp, D.A. Walsh, W. Thielemans, Green one-step synthesis of catalytically active palladium nanoparticles supported on cellulose nanocrystals. ACS Sustain. Chem. Eng. 2 (2014) 1241–1250.

[11] W. Wang, T.J. Zhang, D.W. Zhang, H.Y. Li, Y.R. Ma, L.M. Qi, Y.L. Zhou, X.X. Zhang, Amperometric hydrogen peroxide biosensor based on the immobilization of heme proteins on gold nanoparticles-bacteria cellulose nanofibers nanocomposite, Talanta 84 (2011) 71–77.

[12] H.M.C. Azeredo, M.F. Rosa, L.H.C. Mattoso, Nanocellulose in bio-based food packaging applications, Ind. Crops Prod. 97 (2017) 664–671.

[13] S. Chernousova, M. Epple, Silver as antibacterial agent: Ion, nanoparticle, and metal. Angew. Chem. Int. Ed. 52(2013) 1636−1653.

[14] M. Wu, S. Kuga, Y. Huang, Quasi-one-dimensional arrangement of silver nanoparticles templated by cellulose microfibrils, Langmuir 24 (2008) 10494–10497.

[15] J. Wu, Y. Zheng, W. Song, J. Luan, X. Wen, Z. Wu, X. Chen, Q. Wang, S. Guo, In situ synthesis of silver-nanoparticles/bacterial cellulose composites for slow-released antimicrobial wound dressing, Carbohydr. Polym. 102(2014) 762–771.

[16] A.R.Lokanathan, K.M.A.Uddin, O.J.Rojas, J. Laine, Cellulose nanocrystal-mediated synthesis of silver nanoparticles: Role of sulfate groups in nucleation phenomena, Biomacromolecules 15 (2014) 373−379.

[17] M.S. Wang, F. Jiang, Y.L. Hsieh, N. Nitin, Cellulose nanofibrils improve dispersibility and stability of silver nanoparticles and induce production of bacterial extracellular polysaccharides, J. Mater. Chem. B 2 (2014) 6226–6235.

[18] Z. Shi, J. Tang, L. Chen, C. Yan, S. Tanvir, W.A. Anderson, R.M. Berry, K.C. Tam, Enhanced colloidal stability and antibacterial performance of silver nanoparticles/cellulose nanocrystal hybrids, J. Mater. Chem. B 3 (2015) 603–611.

[19] S. Ifuku, M. Tsuji, M. Morimoto, H. Saimoto, H. Yano, Synthesis of silver nanoparticles templated by TEMPO-mediated oxidized bacterial cellulose nanofibers, Biomacromolecules 10 (2009) 2714–2717.

[20] N. Drogat, R. Granet, V. Sol, A. Memmi, N. Saad, C. Klein Koerkamp, P. Bressollier, P. Krausz, Antimicrobial silver nanoparticles generated on cellulose nanocrystals, J. Nanopart. Res. 13 (2011) 1557–1562.

[21] J. Li, L. Kang, B. Wang, K. Chen, X. Tian, Z. Ge, J. Zeng, J. Xu, W. Gao, Controlled release and long-term antibacterial activity of dialdehyde nanofibrillated cellulose/silver nanoparticle composites, ACS Sustain. Chem. Eng. 7 (2019) 1146−1158.

[22] H. Liu, J. Song, S. Shang, Z. Song, D. Wang, Cellulose nanocrystal/silver nanoparticle composites as bifunctional nanofillers within waterborne polyurethane, ACS Appl. Mater. Inter. 4 (2012) 2413−2419.

[23] H. Yu, B. Sun, D. Zhang, G. Chen, X. Yanga, J. Yao, Reinforcement of biodegradable poly(3-hydroxybutyrate-co-3-hydroxyvalerate) with cellulose nanocrystal/silver nanohybrids as bifunctional nanofillers, J. Mater. Chem. B2 (2014) 8479–8489.

[24] A. Errokh, A. Magnin, J.-L. Putaux, S. Boufi, Morphology of the nanocellulose produced by periodate oxidation and reductive treatment of cellulose fibers, Cellulose 25 (2018) 3899−3911.

[25] C. Noguez, Surface plasmons on metal nanoparticles: The influence of shape and physical environment,J. Phys.Chem. C 111 (2007) 3806–3819.

[26] T.G.M. Van de Ven, A. Sheikhi. Hairy cellulose nanocrystalloids: A novel class of nanocellulose, Nanoscale8 (2016) 15101-15114

[27] D. V. Goia, E. Matijevic, Preparation of monodispersed metal particles. New J. Chem. 22 (1998) 1203–1215.

[28] U.J. Kim, S. Kuga, M. Wada, T. Okano, T. Kondo, Periodate oxidation of crystalline cellulose, Biomacromolecules 1 (2000) 488–492.

[29] S. Vicini, E. Princi, G. Luciano, E. Franceschi, E. Pedemonte, D. Oldak, H. Kaczmarek, A. Sionkowska, Thermal analysis and characterisation of cellulose oxidised with sodium cellulose methaperiodate, Thermochim.Acta. 41(2004)123–130.

[30] A. Dufresne, Nanocellulose: a new ageless bionanomaterial, Mater. Today 16 (2013) 220–227.

[31] S. Pal, Y.K. Tak, J.M. Song, Does the antibacterial activity of silver nanoparticles depend on the shape of the nanoparticle? A study of the gram-negative bacterium *Escherichia coli*, Appl. Environ. Microbiol. 73 (2007)1712–1720.

[32] C. Marambio-Jones, E. M. V. Hoek, A review of the antibacterial effects of silver nanomaterials and potential implications for human health and the environment, J. Nanopart. Res. 12 (2010)1531–1551.

[33] B. Le Ouay, F. Stellacci, Antibacterial activity of silver nanoparticles: A surface science insight, Nano Today10 (2015) 339–354.

[34] P.L. Drake, K.J. Hazelwood, Exposure-related health effects of silver and silver compounds: a review. Ann. Occup. Hyg. 49 (2005) 575–585.

[35] A. Haider, S. Haider, I.K. Kang, A. Kumar, M. Rao Kummara, T. Kamal, S.S. Han, A novel use of cellulose based filter paper containing silver nanoparticles for its potential application as wound dressing agent, Int. J. Biol. Macromol. 108 (2018) 455–461.

[36] A. L. Barry, M. B. Coyle, C. Thorns Berry, E. H. Gerlach, R.W. Hawkinson, Methods of measuring zones of inhibition with the Bauer-Kirby disk susceptibility test. J. Clin. Microbiol. 10 (1979), 885–889.